Intermetallics 115 (2019) 106612

Contents lists available at ScienceDirect

Intermetallics

journal homepage: www.elsevier.com/locate/intermet

Effect of Re on microstructure and mechanical properties of γ/γ′ Co-Ti-based superalloys

Lingling Li[a], Cuiping Wang[a,*], Yuechao Chen[a], Shuiyuan Yang[a], Mujin Yang[a], Jinbin Zhang[a], Yong Lu[a], Jiajia Han[a], Xingjun Liu[b,c,a,**]

[a] College of Materials and Fujian Provincial Key Laboratory of Materials Genome, Xiamen University, Xiamen, 361005, PR China
[b] State Key Laboratory of Advanced Welding and Joining, Harbin Institute of Technology, Harbin, 150001, PR China
[c] Institute of Materials Genome and Big Data, Harbin Institute of Technology, Shenzhen, 518055, PR China

ARTICLE INFO

Keywords:
Co-based superalloys
Mechanical properties
$L1_2$ compound
Microstructure
Lattice parameter misfits
Coarsening behavior

ABSTRACT

Three compositions of Re containing Co-Ti-based alloys with γ/γ′ two-phase microstructure were obtained based on the determined phase relationship in the Co-rich corner at 800 °C. The effect of Re on microstructure, elemental partition behavior, thermodynamic properties, lattice parameter misfits, mechanical properties and γ′ coarsening behavior of the Co-Ti-Re alloys were investigated. The γ/γ′ lattice parameter misfit of the alloys decreases from 0.72% to 0.50%, and the γ′ coarsening rate constant K of alloys decreases from 0.30×10^{-27} $m^3 s^{-1}$ to 0.073×10^{-27} $m^3 s^{-1}$ as Re content increasing form 1 at. % to 5 at. %. Additionally, the volume fraction of γ′ phase ($V_{\gamma'}$) increases from 42.15% to 53.19% and the γ′ solvus temperature increases from 1059 °C to 1085 °C ($T_{solvus\text{-}\gamma'}$) with increasing Re content. Moreover, the 0.2% flow stresses and the 0.2% specific flow stresses of all three alloys exhibit negative temperature dependence at the temperatures ranging from room temperature to 900 °C. And both the 0.2% flow stresses and the 0.2% specific flow stresses increase with the Re content.

1. Introduction

Co-based alloys possess some advantageous properties, such as excellent corrosion resistance and high melting point [1–3]. Thus, Co-based alloys are widely used in industrial fields including gas turbine industries, petrochemical industries, and nuclear power plants etc.

Since Sato et al. reported the outstanding performance of the γ/γ′ two-phase Co–Al–W alloy in 2006 [4], γ′-strengthen Co-based superalloys have attracted researchers' attention. But the γ′ phase in Co–Al–W ternary was metastable [5]. It needs to incorporate many other elements like Ni, Ti, Ta, B, etc. to improve its thermal stability [6–8]. Moreover, as the strength to weight ratio is crucial, the high density (9.45 g cm^{-3} [4]) makes the Co–Al–W alloy unattractive for applications. Then, some researchers paid attention to other Co-base systems [9–11]. The γ′-Co_3Ti is a stable phase and has advantages of low density and high ductility [12–18]. However, the application of the Co_3Ti phase is limited due to its disadvantages of low volume fractions, high γ/γ′ lattice parameter mismatch [19–21]. Recently, some researchers tried to alloy other elements such as V and Cr in the Co-Ti-based system to improve the microstructure stability and mechanical property [22–25]. The results showed that the Co–Ti–Cr alloy [22] and Co–Ti–V alloy [25] have good performance at high temperature range (800–1000 °C). Even though, their strengths were still much less than that of the Ni-based superalloys at whole temperature ranging from room temperature to high temperature. It would greatly limit the wide use of the Co-Ti-based alloys. Thus, the further studies in the Co-Ti-X superalloys are required.

Re is another important alloying element in superalloys, which can change significantly the performance of materials even at a low concentration in the alloys. Re is reported to partition in the γ phase and have a very effective solid solution strengthening that can improve creep resistance in the Ni-based alloys [26–32]. But the effect of Re on the Co-based superalloys is limited. The research results by Kolb et al. [33] and Volz et al. [34] showed that there is no improvement in the creep properties of a single crystalline Co–Ni–Al–W based alloy by Re addition. But Pandey et al. [35] found that an addition of 2 at. % Re to a Co–30Ni–10Al–5Mo–2Nb alloy could reduce the γ/γ′ lattice misfit and improve the microstructure stability. They also investigated the effect of Re in the coarsening behavior, and the experiment results showed that the coarsening rate constant K of the alloy containing 2 at. % Re is

* Corresponding author.
** Corresponding author. State Key Laboratory of Advanced Welding and Joining, Harbin Institute of Technology, Harbin, 150001, PR China.
E-mail addresses: wangcp@xmu.edu.cn (C. Wang), lxj@xmu.edu.cn (X. Liu).

https://doi.org/10.1016/j.intermet.2019.106612
Received 18 July 2019; Received in revised form 16 September 2019; Accepted 16 September 2019
Available online 26 September 2019

1.13×10^{-27} $m^3 s^{-1}$ at 900 °C, which are comparable with the Co–Al–W based superalloys.

In this study, three Co-Ti-Re alloys with different Re content in γ/γ′ two-phase region were prepared based on the determined phase relationship in the Co-rich corner at 800 °C, and the influence of Re in microstructure, elemental partition behavior, thermodynamic properties, γ/γ′ lattice misfits, mechanical properties and γ′ coarsening behavior of the Co-Ti-Re alloys were investigated.

2. Experimental procedures

Experimental alloys with 200 g in weight were melted from high-purity metals (Co: 99.9 wt %, Ti: 99.9 wt %, Re: 99.9 wt %) in a vacuum induction furnace. The alloys were melted for 5 times to achieve the composition homogeneity. Then the specimens were put into quartz capsules and filled with argon gas to prevent from oxidation.

To acquire the information of phase relationship, the encapsulated specimens were annealed at 800 °C for 2880 h (h) and then quenched into ice water. To obtain the best heat treatment parameter for mechanical properties and investigate the coarsening behavior of γ′ phase, specimens cut from ingots were solution-treated at 1100 °C for 48 h (argon atmosphere). And then specimens were annealed at 800 °C for various times (0, 8 h, 16 h, 24 h, 48 h, 72 h, 100 h, 200 h, 300 h, 400 h, 600 h).

Specimens were mechanically polished and then etched in a solution of HNO_3 (vol.40%) + HCl (vol. 40%) + H_2O (vol. 20%) for a few seconds before microstructural observations. Backscatter-electron (BSE) images were taken by electron probe microanalyzer (EPMA) (JXA-8100R, JEOL, Japan) operated at a 20.0 kV accelerating voltage and a 1.0×10^{-8} A probe current. Secondary electron images were taken by scanning electron microscope (SEM) (SU-70, Hitachi, Ibaraki, Japan) operated at a 10 kV accelerating voltage. The volume fraction and sizes of γ′ phase were calculated by software Image-Pro Plus 6.0. Phase compositions were determined by Wavelength Dispersive Spectrometer (WDS). X-ray diffraction (XRD) (Bruker Daltonic Inc., Billerica, MA, USA) was performed for evaluation of γ/γ′ lattice misfits using a Cu Kα radiation at 40 kV and 40 mA. Then the curves were fitted using the technical graphing and data analysis software Jade 6.0. Differential scanning calorimetry (DSC) (NETZSCH DSC 404, NETZSCH, Selb, German) was used to determine the transition temperatures of the alloys, under argon atmosphere at a heating rate of 10 °C·s^{-1}.

To measure the hardness of samples, Vickers micro hardness tester (HMV-2, Shimadzu, Kyoto, Japan) were used with a load of 4.9 N. For the compression tests, the samples were cut into the cylinder-shape (ϕ 4 mm × 6 mm) by wire-cutting machine. The 0.2% flow stresses were determined from compressive tests at 25 °C, 600 °C, 700 °C, 800 °C, 850 °C, and 900 °C at a strain rate of 10^{-4} s^{-1}.

3. Results and discussion

3.1. Phase relationship and composition design

The experimentally determined phase relationship of the Co-Ti-Re system in the Co-rich corner at 800 °C and typical back-scattered-electron (BSE) images of equilibrium microstructure are shown in Fig. 1. The two-phase and three-phase equilibria are characterized by different symbols. The equilibrium compositions in the Co-rich corner of the Co-Ti-Re ternary system at 800 °C are shown in Table 1. The equilibrium compositions of phases in alloy $Co_{79}Ti_{11}Re_{10}$ show that the solubility of Re in the γ′-Co_3Ti phase and γ-(αCo) phase is 5.9% and 6.5% at 800 °C, respectively.

According to the above results shown in Fig. 1 and Table 1, three alloys $Co_{87}Ti_{12}Re_1$ (Re1), $Co_{85}Ti_{12}Re_3$ (Re3), $Co_{83}Ti_{12}Re_5$ (Re5) were all in the γ/γ′ two-phase region at 800 °C. Thus, in order to acquire the Co-Ti-Re ternary alloy with γ/γ′ two-phase microstructure, and to study the effect of element Re, the alloys Re1, Re3, and Re5 were solutionized at 1100 °C to obtain the single γ phase, and then aged at 800 °C to precipitate γ′ phase.

The equilibrium compositions of γ-αCo in alloys Re1, Re3 and Re5 were determined as Co-6.5Ti-1.2Re, Co-6.2Ti-3.3Re and Co-5.8Ti-5.3Re (at.%), while the equilibrium compositions of γ′-Co_3Ti were determined as Co-20.3Ti-0.8Re, Co-19.5Ti-2.5Re and Co-18.5Ti-4.5Re (at. %), as listed in Table 1. The partitioning parameter K_X is described as $K_X = C_{\gamma'}/C_{\gamma}$ ($C_{\gamma'}$ and C_{γ} represent the equilibrium composition of element X in γ′ and γ phases). The element X tends to distribute into the γ′ phase if $K_X > 1$, while prefers to partition into the γ phase if $K_X < 1$. All three alloys Re1, Re3, and Re5 exhibited the K_{Re} with the value of 0.67, 0.76, and 0.85, respectively. Re is confirmed as a γ former in the present Co-Ti-Re ternary system. Re is different with respect to other alloying additions such as Nb, Ta, and V, which concentrate in the γ′ phase in Co-Ti-based alloys.

3.2. Microstructure and lattice parameter misfit

Fig. 2a–c shows the typical SEM images of alloys Re1, Re3, and Re5 after aging at 800 °C for 24 h. All three alloys show a homogeneous distribution of cubic γ′ precipitates within the γ matrix. And there is no other coarsening phase at the grain boundary. The sizes of γ′ precipitates in the alloys Re1, Re3, and Re5 were measured as 64.4 ± 0.7 nm, 45.5 ± 0.6 nm, and 42.1 ± 0.4 nm, respectively, as shown in Table 3.

The lattice parameter misfit δ is an critical parameter of γ′ strengthened superalloys and it can be calculated by equation (1) [36]:

$$\delta = 2(a_{\gamma'} - a_{\gamma})/(a_{\gamma'} + a_{\gamma}) \quad (1)$$

Estimation of an equivalent cubic lattice parameter $a_{\gamma'}$ for the γ′ phase and a_{γ} for the γ phase is shown in Ref. [36]. The X-ray diffraction (002) peaks of the alloys Re1-Re5 after solutioning at 1100 °C for 48 h and then ageing at 800 °C for 24 h are shown in Fig. 2d–f. The lattice parameter misfits of alloys Re1, Re3, and Re5 were calculated and shown in Table 2. For alloy Re1, the equivalent cubic lattice parameter $a_{\gamma'}$ is about 3.595 Å, and $a_{\gamma}$is about 3.569 Å, so the lattice misfit δ is about 0.72%. When the Re content increases to 5 at. % for alloy Re5, both the cubic lattice parameters $a_{\gamma'}$ and a_{γ}increase to about 3.642 Å and 3.624 Å respectively, with the reduction in γ/γ′ lattice misfit value to about 0.50%. As shown in Fig. 3, Both the lattice parameters of γ phase and γ′ phase are enhanced with increasing Re content. As Re is enriched in the γ phase, the lattice distortion of γ phase increases more than that of γ′ phase, thus the lattice parameter misfits decrease with increasing Re content.

It is found that Re is effective in reducing the lattice parameter misfit compared to the binary Co–Ti alloys, which were reported to have values of 0.75–1.67% in Refs. [22,36]. Additionally, the lattice parameter misfit of the alloy Re5 is lower than that of Co–11Ti–15Cr alloy (0.54%) [22] and Co–9Al–9W alloy (0.53%) [4]. Both Re and Cr are γ phase formers which preferentially partitions into the γ phase.

In new γ/γ′ strengthen Co-based alloys [22,36], the volume fraction of the γ′ precipitates ($V_{\gamma'}$) is another essential factor. Mostly, the high $V_{\gamma'}$ corresponds to the high creep strength of the superalloys. Fig. 4 shows the plots of $V_{\gamma'}$ versus the aging time in the alloys Re1-Re5 at 800 °C. The $V_{\gamma'}$ of the γ′ precipitates were 42.15%, 47.96% and 53.19% in the Re1, Re3 and Re5 alloys when ageing at 800 °C for the 24 h, respectively. It indicates that the $V_{\gamma'}$ of the alloys increases as Re content increasing.

3.3. Effect of Re on the phase transition temperature, hardness, and density

3.3.1. Phase transition temperature

DSC heating curves of all three alloys Re1-Re5 are shown in Fig. 5a. The $T_{solvus\text{-}\gamma'}$ referres to the γ′ solvus temperature, and T_m referres to the melting temperature of the alloy. The $T_{solvus\text{-}\gamma'}$ of alloys Re1, Re3, and

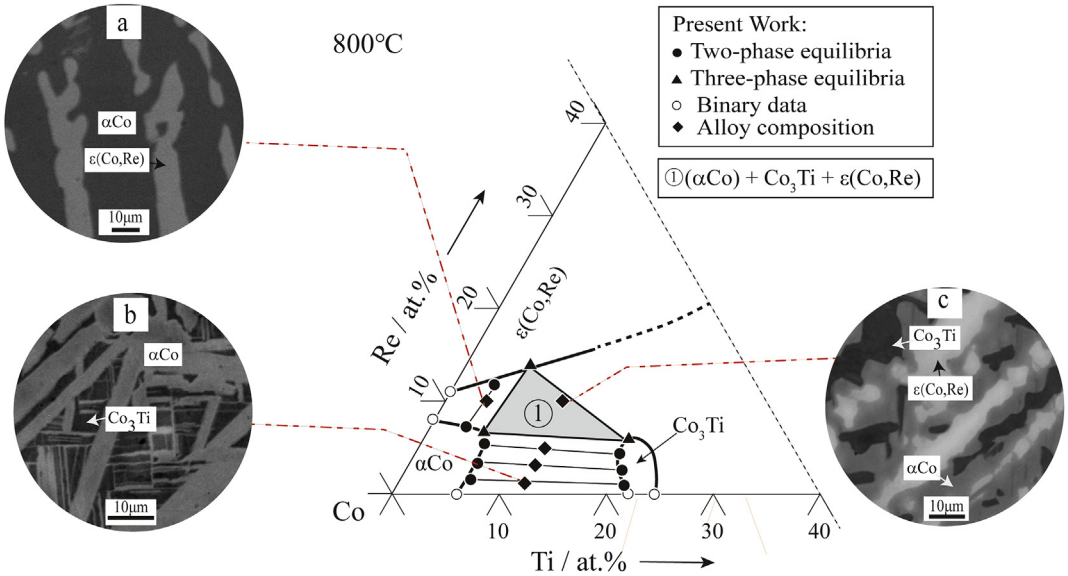

Fig. 1. Experimentally determined isothermal section of the Co–Ti-Re system in the Co-rich corner at 800 °C and typical equilibrium microstructure images: (a) BSE image of alloy $Co_{86}Ti_4Re_{10}$; (b) BSE image of alloy $Co_{87}Ti_{12}Re_1$; (c) BSE image of alloy $Co_{79}Ti_{11}Re_{10}$.

Table 1
Equilibrium compositions in the Co-rich corner of the Co-Ti-Re ternary alloys at 800 °C.

Acronym	Alloys (at. %)	Equilibria	Composition (at. %)					
		Phase 1/Phase 2/Phase 3	Phase 1		Phase 2		Phase 3	
			Re	Ti	Re	Ti	Re	Ti
Re1	$Co_{87}Ti_{12}Re_1$	αCo/Co_3Ti	1.2	6.5	0.8	20.3	–	–
Re3	$Co_{85}Ti_{12}Re_3$	αCo/Co_3Ti	3.3	6.2	2.5	19.5	–	–
Re5	$Co_{83}Ti_{12}Re_5$	αCo/Co_3Ti	5.3	5.8	4.5	18.5	–	–
—	$Co_{79}Ti_{11}Re_{10}$	αCo/Co_3Ti/ε(Co,Re)	6.5	5.5	5.9	19.1	13.9	6.1
—	$Co_{86}Ti_4Re_{10}$	αCo/ε(Co,Re)	7.2	3.2	11.9	3.8	–	–

Table 2
The calculated lattice parameter misfits of alloys Re1-Re5.

Alloys	lattice parameter $a_{\gamma'}$ (Å)	lattice parameter a_{γ}(Å)	lattice parameter misfit δ (%)
Re1	3.595 ± 0.0003	3.569 ± 0.0002	0.72 ± 0.01
Re3	3.635 ± 0.0003	3.614 ± 0.0004	0.58 ± 0.02
Re5	3.642 ± 0.0001	3.624 ± 0.0003	0.50 ± 0.01

Re5 are about 1059 °C, 1073 °C, and 1085 °C, respectively. The T_m of alloys Re1, Re3, and Re5 are about 1203 °C, 1214 °C, and 1222 °C, respectively. It indicates that both the $T_{solvus\text{-}\gamma'}$ and T_m of alloys increase as Re content increasing. The comparison of alloys Re1, Re3, Re5 with other Co-based superalloys is shown in Fig. 5b. The $T_{solvus\text{-}\gamma'}$ of alloys Re1, Re3, Re5 are higher than that of Co–12Ti, Co–9Al–9W, Co–12Ti–4V, except Co–11Ti–15Cr. Especially, the $T_{solvus\text{-}\gamma'}$ of alloys Re1, Re3, Re5 are higher than that of Co–12Ti ($T_{solvus\text{-}\gamma'}$: 1022 °C) [36] by about 37 °C, 51 °C, and 63 °C, respectively. Moreover, the $T_{solvus\text{-}\gamma'}$ of alloys Re1, Re3, Re5 are higher than that of Co–9Al–9W ($T_{solvus\text{-}\gamma'}$: 1000 °C) [4] by about 59 °C, 73 °C, and 85 °C, respectively.

3.3.2. Hardness

The aging time dependence of the Vickers hardness of alloys Re1-Re5 are shown in Fig. 6. All three hardness curves of alloys Re1-Re5 exhibit a rapid rising from 0 to 24 h, then have a slowly falling until 100 h aged at 800 °C. Thus, the alloys for compression tests in the present work were aged at 800 °C for 24 h. The peak hardness of the alloys Re1, Re3 and Re5 were 428 Hv4.9, 515 Hv4.9 and 525 Hv4.9 when ageing at 800 °C for 24 h respectively. The Vickers hardness of all

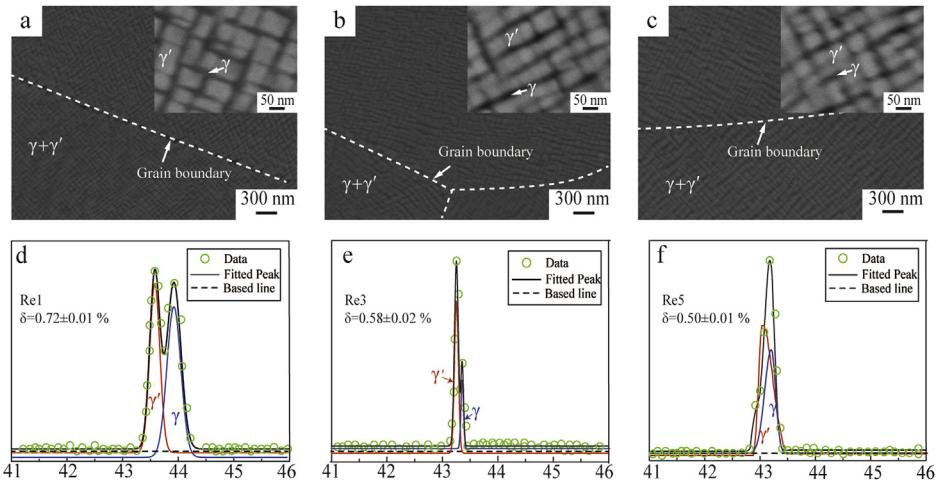

Fig. 2. SEM images and X-ray diffraction (002) peaks obtained from the alloys: (a) SEM images of alloy Re1 aged at 800 °C for 24h; (b) SEM images of alloy Re3 aged at 800 °C for 24h; (c) SEM images of alloy Re5 aged at 800 °C for 24h; (d) X-ray diffraction (002) for alloy Re1 aged at 800 °C for 24h; (e) X-ray diffraction (002) for alloy Re3 aged at 800 °C for 24h; (f) X-ray diffraction (002) for alloy Re5 aged at 800 °C for 24h.

Table 3
Average size of γ′ precipitates in the alloys Re1-Re5 after aging at 800 °C for various time.

Acronym	Alloys (at. %)	Average size of γ′ precipitates aging for various time (nm)						
		8 h	16 h	24 h	100 h	200 h	300 h	400 h
Re1	$Co_{87}Ti_{12}Re_1$	37.9 ± 0.4	44.6 ± 0.5	64.4 ± 0.7	102.1 ± 1.3	118.7 ± 1.8	/	/
Re3	$Co_{85}Ti_{12}Re_3$	31.0 ± 0.4	42.3 ± 0.4	45.5 ± 0.6	68.3 ± 0.6	79.6 ± 0.8	92.8 ± 1.1	105.9 ± 1.6
Re5	$Co_{83}Ti_{12}Re_5$	25.2 ± 0.3	34.7 ± 0.4	42.1 ± 0.4	62.3 ± 0.5	76.6 ± 0.7	83.3 ± 1.0	96.6 ± 1.2

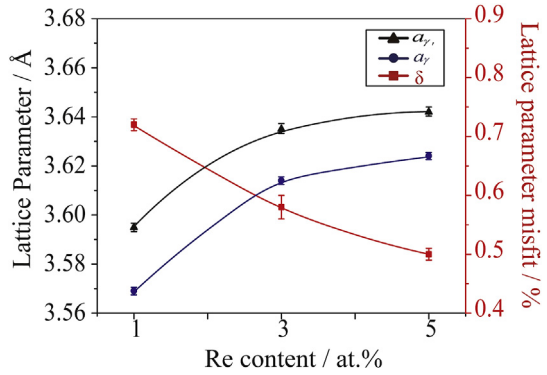

Fig. 3. The lattice parameters of γ, γ′ phase and the lattice parameter misfits in the alloys Re1-Re5.

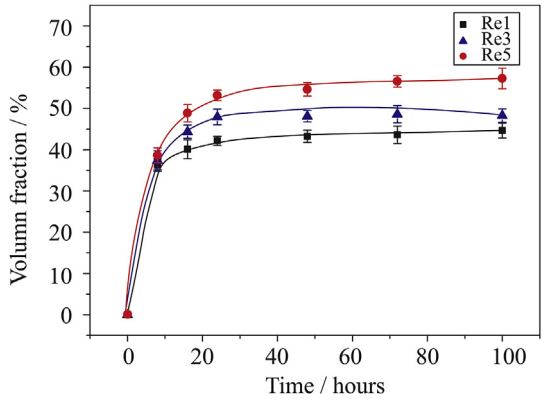

Fig. 4. Aging time dependence of $V_{\gamma'}$ in the alloys Re1-Re5 at 800 °C.

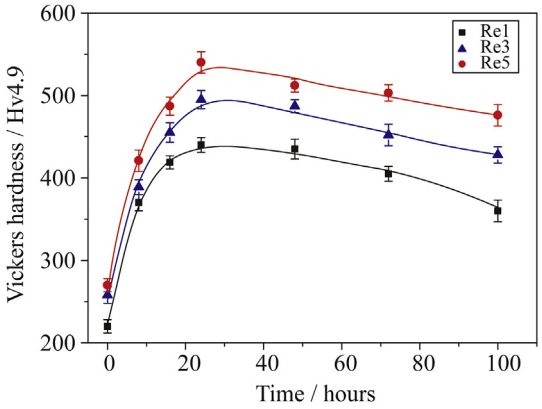

Fig. 6. Aging time dependence of hardness in the alloys Re1-Re5 at 800 °C.

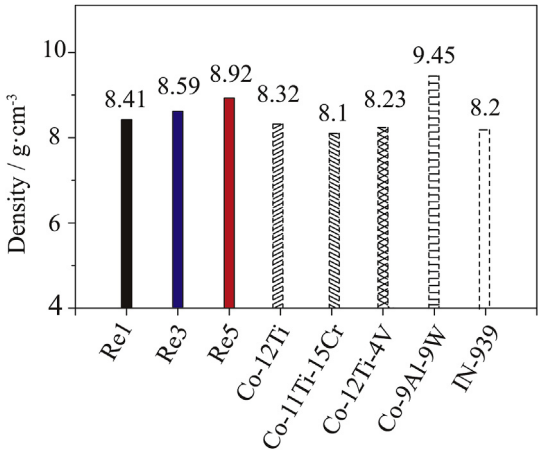

Fig. 7. Comparison of the densities of alloys Re1, Re3, Re5, Co–12Ti [22], Co–11Ti–15Cr [22], Co–12Ti–4V [25], Co–9Al–9W [4], and IN 939 [1].

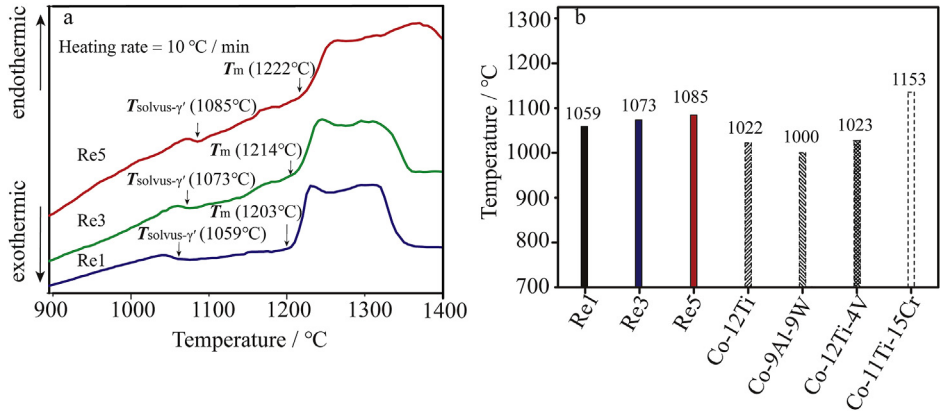

Fig. 5. (a) DSC heating curves of the alloys Re1-Re5; (b) Comparison of $T_{solvus-\gamma'}$ of alloys Re1, Re3, Re5, Co–12Ti [36], Co–9Al–9W [4], Co–12Ti–4V [25], and Co–11Ti–15Cr [22].

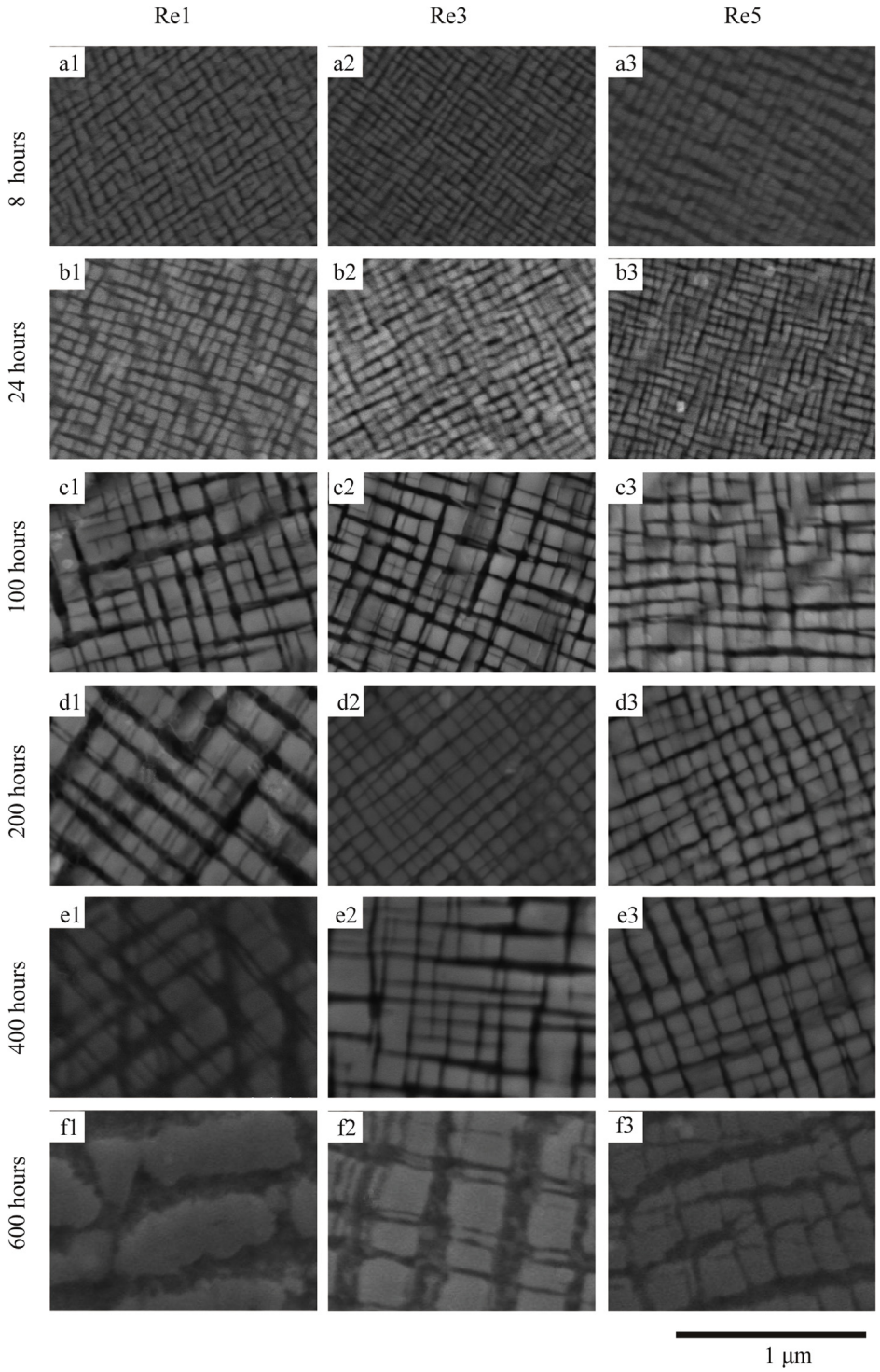

Fig. 8. Typical microstructure of precipitates in alloys Re1-Re5 after aging at 800 °C for different times: (a) 8 h, (b) 24 h, (c) 100 h, (d) 200 h, (e) 400 h, (f) 600 h.

three alloys are higher than that of Co–9Al–9W (~400) [4].

3.3.3. Density

The densities of alloys Re1, Re3, Re5, and other Co-based alloys for comparison are shown in Fig. 7. The densities of alloys Re1, Re3 and Re5 were determined to be 8.41 g cm^{-3}, 8.59 g cm^{-3}, and 8.92 g cm^{-3} respectively. By adding Re, the densities of alloys are increasing compared to the density of the alloy Co–12Ti (8.32 g cm^{-3}) [22]. As shown in Fig. 7, all the densities of alloys Re1, Re3 and Re5 are higher than that of Co–11Ti–15Cr (8.1 g cm^{-3}) [22], Co–12Ti–4V (8.23 g cm^{-3}) [25], and IN 939 (8.2 g cm^{-3}) [1]. However, the highest density of the alloy Re5 in our test is still much lower than that of Co–9Al–9W alloy (9.45 g cm^{-3} [4]).

3.4. Coarsening behavior

For microstructure evolution, the alloys Re1, Re3, and Re5 were solutionized at 1100 °C for 48 h and then aged at 800 °C for 8 h, 24 h, 100 h, 200 h, 400 h, 600 h. The typical SEM microstructures of the alloys Re1-Re5 after aging at 800 °C for various time are shown in Fig. 8.

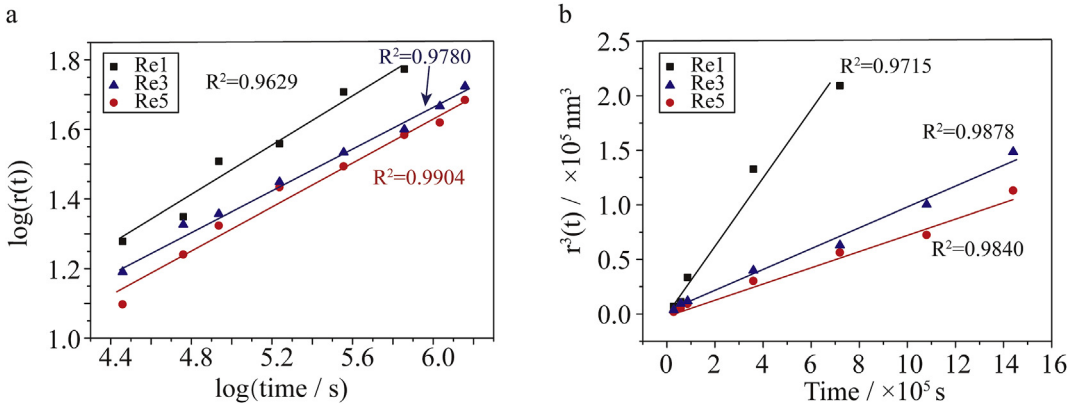

Fig. 9. Coarsening kinetics of the alloys Re1-Re5 aged at 800 °C: (a) the plots of $\log\frac{r^3(t)}{r^3(0)}$ versus log(t); (b) the plots of $r^3(t) - r^3(0)$ versus the aging time.

The bright cubic phase is γ′, and the dark phase is γ. There are obvious differences in the microstructural evolution among the three alloys. For the alloy Re1, the coalescence of γ′ precipitates was lost at the γ/γ′ interfaces after ageing for 400 h as shown in Fig. 8 e1. For the alloys Re3 and Re5, the morphology of γ′ precipitates was irregular when ageing for 600 h as shown in Fig. 8 f1 and f2.

As reported by Refs. [37–42], in LSW theory, when the coarsening behavior of precipitate is controlled by the diffusion of solute in the matrix, the growth of precipitate follows a third power as a function of aging time as shown in equation (2):

$$r^3(t) - r^3(0) = Kt \quad (2)$$

In equation (2), r (0) represents the initial equivalent precipitate radius, r(t) represents the instantaneous equivalent precipitate radius, and K represents the coarsening rate coefficient. If the precipitates are cubic, r was replaced by $\bar{a}/2$, where $\bar{a}$ is the average edge length of precipitates [42].

The average γ′ precipitate sizes $\bar{a}$ in the alloys Re1-Re5 after aging at 800 °C for various time are shown in Table 3. The base 10 logarithm of the equivalent precipitate radius r(t) versus the logarithm of time for the different aging time periods at 800 °C have been plotted in Fig. 9a. By linear fittings, the power exponents were calculated to be 0.37, 0.32 and 0.29 for the Re1, Re3 and Re5 alloys respectively. Thus, the coarsening rates of the alloys Re1-Re5 have the 1/3 power law exponents that agree with LSW theory. This indicates that the coarsening rates of γ′ precipitates in alloys Re1-Re3 are controlled by diffusion.

Then the plots of $r^3(t)$ versus the aging time in alloys Re1, Re3, and Re5 were shown in Fig. 9b. The slopes of the linear fits gave the coarsening rate constant, K, for the Re1, Re3 and Re5 alloys to be 0.30×10^{-27}, 0.096×10^{-27} and 0.073×10^{-27} $m^3 s^{-1}$, respectively. The Re1 alloy had the fastest rate, while the Re5 alloy was the slowest. The results indicate that adding Re content can reduce the coarsening rate of the γ′ precipitates. Meher et al. [43] measured the coarsening rate K of Co–10Al–10W at 800 °C to be 0.07×10^{-27} $m^3 s^{-1}$. Chellman et al. [44] investigated the coarsening behavior of the Ni-19.3 at.% Al alloy and measured K to be 1.3×10^{-27} $m^3 s^{-1}$ at 800 °C. Both the coarsening rates of alloy Re3 and Re5 are slower than the Ni-19.3 at.% Al alloy. And the slowest coarsening rate of alloy Re5 in our results is comparable to the Co–10Al–10W alloy. P. Pandey [35] and W.Z. Wang [45] et al. also reported that the coarsening rates of γ′ precipitates were restrained by adding Re. Firstly, the segregation of Re in the γ matrix causes the slow diffusivity. Secondly, the reduction of γ/γ′ lattice parameter misfit has a weakening effect on the elastic strain energy of γ/γ′ interface.

3.5. Mechanical properties

The 0.2% flow stresses plots of the Re1, Re3 and Re5 alloys versus the temperature after solutioning at 1100 °C for 48 h and then ageing at 800 °C for 24 h are shown in Fig. 10a. For comparison, Fig. 10a also provided the 0.2% flow stresses curves of Co–12Ti (compression tests) [36], Co–12Ti–4V (compression tests) [25], Co–11Ti–15Cr (compression tests) [22], Co–9Al–9W (compression tests) [46] and IN-939 (tensile tests) [1]. Mostly, the 0.2% flow stresses plots of Co-based superalloys demonstrate the anomalous phenomenon that the flow stresses increase rather than decrease when the temperature rises from ~600–850 °C [22–25]. It is widely accepted as one of the explanations that the activation of the cross-slip pinning process when a sufficient number of dislocation pairs are trapped inside the ordered precipitates [47]. But, the flow stresses of alloys Re1-Re5 exhibit negative temperature dependence during the whole test temperatures ranging from room temperature to 900 °C. This phenomenon was similarly to the research by Makineni et al. [48], who explained that the dislocation pair move through the precipitate and escape without any accumulation inside the ordered precipitate because of the small ordered cuboidal precipitates with sizes < 50 nm. In this study, the sizes of γ′ precipitates in the alloys Re1-Re5 are 42–64 nm, which is far smaller than the reported Co-based alloys [22–25]. The flow stresses of alloys Re1, Re3, and Re5 are 816 MPa, 919 MPa, and 995 MPa at room temperature respectively. The results agree with the hardness test. It shows that the flow stresses exhibit positive dependence with the Re content. It may be explained by follows: the γ′ volume fraction increases and γ/γ′ lattice misfit decreases with the Re content. The 0.2% flow stresses of alloys Re1-Re5 demonstrate good performance ranging from room temperature to 700 °C, exceeding Co–9Al–9W [46], Co–12Ti–4V [25], Co–11Ti–15Cr [22] and Co–12Ti [36]. Above 700 °C, the 0.2% flow stresses of the alloys Re1-Re5 are still higher than Co–9Al–9W [46] and Co–12Ti [36]. The 0.2% flow stresses of the alloys Re3 and Re5 are comparable with that of the Co–11Ti–15Cr [22], Co–12Ti–4V [25], and IN 939 [1] at temperature ranging from 800 °C to 900 °C.

As the densities of alloys Re1, Re3 and Re5 were determined above, the 0.2% specific flow stress curves of alloys Re1-Re5 and alloys for comparison versus temperature are shown in Fig. 10b. It shows the same tendency when the 0.2% flow stresses normalized by the densities. The 0.2% specific flow stresses of alloys Re1, Re3, and Re5 are about 100 MPa/g·cm^{-3}, 107 MPa/g·cm^{-3}, 111 MPa/g·cm^{-3} at room temperature, respectively. Although the densities of Re1, Re3 and Re5 alloys are higher than Co–12Ti (8.32 g cm^{-3} [22]), Co–11Ti–15Cr (8.1 g cm^{-3} [22]), Co–12Ti–4V (8.23 g cm^{-3} [25]), the alloys Re1-Re5 exhibit the great 0.2% specific flow stresses at temperatures ranging from room temperature to 700 °C. The 0.2% specific flow stresses of Re5 alloy are slightly lower than Co–11Ti–15Cr [22], Co–12Ti–4V [25], and comparable with IN939 [1] at 800–900 °C.

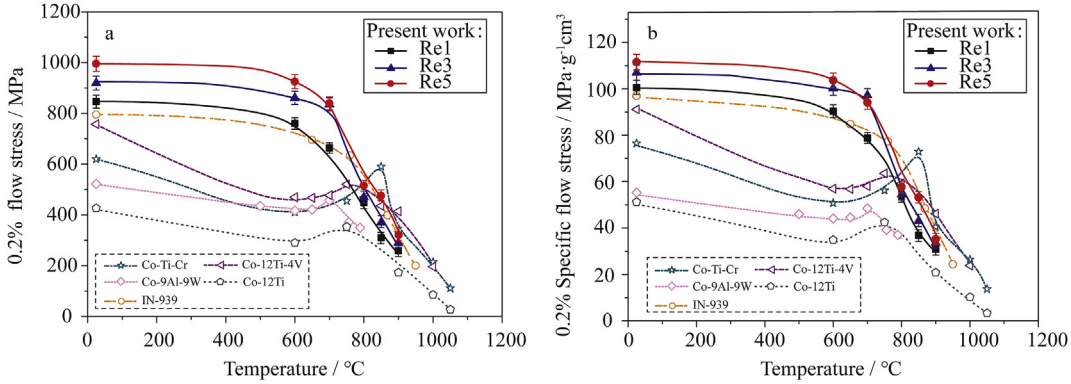

Fig. 10. (a) Comparison of the 0.2% flow stress versus temperature curves of alloys Re1, Re3, Re5 (compression tests), Co–9Al–9W (compression tests) [45], Co–12Ti (compression tests) [36], Co–11Ti–15Cr (compression tests) [22], Co–12Ti–4V (compression tests) [25], and nickel-based alloy IN 939 (tensile tests) [1]. Compositions are given in at.%; (b) Comparison of the 0.2% specific flow stress versus temperature curves of alloys Re1, Re3, Re5, Co–9Al–9W [46], Co–12Ti [36], Co–11Ti–15Cr [22], Co–12Ti–4V [25], and nickel-based alloy IN 939 [1].

4. Conclusions

Three Co-Ti-Re alloys with γ/γ′ two-phase microstructure were obtained based on the determined phase relationship in the Co-rich corner at 800 °C. The effects of Re on the microstructure, partitioning behavior, thermodynamic properties, mechanical properties and γ′ coarsening behavior of the Co-Ti-Re alloys are investigated. The main results are summarized as follows:

1The compositions of γ-αCo were determined as Co-6.5Ti-1.2Re, Co-6.2Ti-3.3Re and Co-5.8Ti-5.3Re (at. %), while the compositions of γ′-Co_3Ti were determined as Co-20.3Ti-0.8Re, Co-19.5Ti-2.5Re and Co-18.5Ti-4.5Re in the alloys Re1, Re3, and Re5, respectively. Re is enriched in the αCo phase.

2The lattice parameter misfits of alloy Re1, Re3, and Re5 when aged at 800 °C for 24 h were 0.72%, 0.58%, and 0.50%, respectively. The volume fractions of the γ′ precipitates in the alloy Re1, Re3, and Re5 when aged at 800 °C for 24 h were 42.15%, 47.96%, and 53.19%, respectively. The lattice parameter misfits of alloys decrease, while the $V_{\gamma'}$ of alloys increases as Re content.

3The γ′ solvus temperatures of alloy Re1, Re3, and Re5 were determined as 1059 °C, 1073 °C, and 1085 °C respectively. The $T_{\text{solvus-}\gamma'}$ of alloys increases as Re content increasing.

4The coarsening rate constants K for the alloys Re1, Re3 and Re5 were measured to be 0.30×10^{-27}, 0.096×10^{-27} and 0.073×10^{-27} $m^3 s^{-1}$, respectively. The coarsening rate constants of alloys decrease with increase in Re content.

5The 0.2% flow stresses of all three alloys show negative temperature dependence and exceed that of Co–12Ti and Co–9Al–9W at the temperatures ranging from room temperature to 900 °C. And the 0.2% flow stresses of all three alloys are higher than that of Co–Ti–V, Co–11Ti–15Cr, and IN939 at the temperatures ranging from room temperature to 700 °C, even normalized by mass densities.

This work was supported by the National Natural Science Foundation of China [Grant No. 51831007] and National Key R&D Program of China [Grant No. 2017YFB0702901].

References

[1] C.T. Sims, N.S. Stoloff, W.C. Hagel, Superalloys II, John Wiley & Sons, New York, 1987, pp. 584–585.
[2] F.S. Pettit, G.H. Meier, M. Gell, C.S. Kartovich, R.H. Bricknel, W.B. Kent, J.F. Radovich, Oxidation and Hot Corrosion of Superalloys, Superalloys (1984) 651–687.
[3] T.M. Pollock, Alloy design for aircraft engines, Natural Materials 15 (8) (2016) 809–815.
[4] J. Sato, T. Omori, K. Oikawa, I. Ohnuma, R. Kainuma, K. Ishida, Cobalt-base high-temperature alloys, Science 312 (5770) (2006) 90–91.
[5] S. Kobayashi, Y. Tsukamoto, T. Takasugi, H. Chinen, T. Omori, K. Ishida, S. Zaefferer, Determination of phase equilibria in the Co-rich Co-Al-W ternary system with a diffusion-couple technique, Intermetallics 17 (12) (2009) 1085–1089.
[6] K. Shinagawa, T. Omori, J. Sato, K. Oikawa, I. Ohnuma, R. Kainuma, K. Ishida, Phase equilibria and microstructure on γ′ Phase in Co-Ni-Al-W system, Mater. Trans. 49 (6) (2008) 1474–1479.
[7] I. Povstugar, P.P. Choi, S. Neumeier, A. Bauer, C.H. Zenk, M. Göken, D. Raabe, Elemental partitioning and mechanical properties of Ti- and Ta-containing Co-Al-W-base superalloys studied by atom probe tomography and nanoindentation, Acta Mater. 78 (4) (2014) 78–85.
[8] K. Shinagawa, T. Omori, K. Oikawa, R. Kainuma, K. Ishida, Ductility enhancement by boron addition in Co-Al-W high-temperature alloys, Scr. Mater. 61 (6) (2009) 612–615.
[9] S.K. Makineni, B. Nithin, A new tungsten-free γ-γ′ Co-Al-Mo-Nb-based superalloy, Scr. Mater. 98 (2015) 36–39.
[10] S.K. Makineni, A. Samanta, T. Rojhirunsakool, T. Alam, B. Nithin, A.K. Singh, R. Banerjee, K. Chattopadhyay, A new class of high strength high temperature Cobalt based γ-γ′ Co-Mo-Al alloys stabilized with Ta addition, Acta Mater. 97 (2015) 29–40.
[11] S.K. Makineni, B. Nithin, D. Palanisamy, K. Chattopadhyay, Phase evolution and crystallography of precipitates during decomposition of new "tungsten-free" Co (Ni)-Mo-Al-Nb γ-γ′ superalloys at elevated temperatures, J. Mater. Sci. 51 (17) (2016) 7843–7860.
[12] J.B. Blaise, P. Viatour, J.M. Drapier, On the stability and precipitation of the Co_3Ti phase in Co-Ti alloys, Cobalt 49 (1970) 192–195.
[13] P. Viatour, J.M. Drapier, D. Coutsouradis, Stability of the gamma prime Co_3Ti compound in simple and complex Co Alloys, Cobalt 3 (1973) 67–74.
[14] J.L. Murray, The Co-Ti (Cobalt-Titanium) system, J. Phase Equilibria 3 (1) (1982) 74.
[15] T. Takasugi, O. Izumi, High temperature strength and ductility of polycrystalline Co_3Ti, Acta Metall. 33 (1) (1985) 39–48.
[16] T. Takasugi, O. Izumi, Recrystallization and grain growth of Co_3Ti, Acta Metall. 33 (1) (1985) 49–58.
[17] T. Takasugi, O. Izumi, Electronic and structural studies of grain boundary strength and fracture in $L1_2$ ordered alloys-I. On binary A_3B alloys, Acta Metall. 33 (7) (1985) 1247–1258.
[18] H.Y. Yasuda, S. Yamamura, Y. Umakoshi, Recrystallization texture in cold-rolled Co_3Ti polycrystals, Scr. Mater. 44 (5) (2001) 765–769.
[19] C. Cui, D. Ping, Y. Gu, H. Harada, A new Co-Base superalloy strengthened by γ′ phase, Mater. Trans. 47 (2006) 2099–2102.
[20] A. Bhowmik, S. Neumeier, S. Rhode, H.J. Stone, Allotropic transformation induced stacking faults and discontinuous coarsening in a γ-γ′ Co-base alloy, Intermetallics 59 (2015) 95–101.
[21] C. Rogister, D. Coutsouradis, L. Habraken, Improvement of heat-resisting cobaltbase alloys by precipitation hardening, Cobalt 34 (1967) 3–9.
[22] C.H. Zenk, I. Povstugar, R. Li, F. Rinaldi, S. Neumeier, D. Raabe, M. Göken, A novel type of Co-Ti-Cr-base γ/γ′ superalloys with low mass density, Acta Mater. 135 (2017) 244–251.
[23] J.J. Ruan, C.P. Wang, C.C. Zhao, S.Y. Yang, T. Yang, X.J. Liu, Experimental investigation of phase equilibria and microstructure in the Co-Ti-V ternary system, Intermetallics 49 (4) (2014) 121–131.
[24] J.J. Ruan, X.J. Liu, S.Y. Yang, W.W. Xu, T. Omori, T. Yang, B. Deng, H.X. Jiang, C.P. Wang, R. Kainuma, Novel Co-Ti-V-base superalloys reinforced by $L1_2$ -ordered γ′ phase, Intermetallics 92 (2018) 126–132.
[25] X.J. Liu, Y.W. Pan, Y.C. Chen, J.J. Han, S.Y. Yang, J.J. Ruan, C.P. Wang, Y.S. Yang, Y.J. Li, Effects of Nb and W additions on the microstructures and mechanical

properties of novel γ/γ′ Co-V-Ti-based superalloys, Metals 8 (7) (2018) 12.
[26] J. Rüsing, N. Wanderka, U. Czubayko, V. Naundorf, D. Mukherji, J. Rösler, Rhenium distribution in the matrix and near the particle-matrix interface in a model Ni-Al-Ta-Re superalloy, Scr. Mater. 46 (3) (2002) 235–240.
[27] S.G. Tian, B.J. Qian, F.S. Liang, A.A. Li, X.F. Yu, Creep behaviors of a single crystal nickel-based superalloy containing 4.2%Re, Mater. Sci. Forum 689 6.
[28] A. Volek, F. Pyczak, R.F. Singer, H. Mughrabi, Partitioning of Re between γ and γ′ phase in nickel-base superalloys, Scr. Mater. 52 (2) (2005) 141–145.
[29] H. Murakami, H. Harada, H.K.D.H. Bhadeshia, The location of atoms in Re- and V-containing multicomponent nickel-base single-crystal superalloys, Appl. Surf. Sci. 76–77 (1994) 177–183.
[30] A.C. Yeh, S. Tin, Effects of Ru and Re additions on the high temperature flow stresses of Ni-base single crystal superalloys, Scr. Mater. 52 (6) (2005) 519–524.
[31] J. Yu, X. Sun, T. Jin, N. Zhao, H. Guan, Z. Hu, Effect of Re on deformation and slip systems of a Ni base single-crystal superalloy, Mater. Sci. Eng. A 458 (1) (2007) 39–43.
[32] R.W. Kozar, A. Suzuki, W.W. Milligan, J.J. Schirra, M.F. Savage, T.M. Pollock, Strengthening mechanisms in polycrystalline multimodal nickel-base superalloys, Metall. Mater. Trans. A 40 (7) (2009) 1588–1603.
[33] M. Kolb, C.H. Zenk, A. Kirzinger, I. Povstugar, D. Raabe, S. Neumeier, M. Göken, Influence of rhenium on γ′- strengthened cobalt-base superalloys, J. Mater. Res. 32 (2017) 2551–2559.
[34] N. Volz, C.H. Zenk, R. Cherukuri, T. Kalfhaus, M. Weiser, S.K. Makineni, C. Betzing, M. Lenz, B. Gault, S.G. Fries, J. Schreuer, R. Vaßen, S. Virtanen, D. Raabe, E. Spiecker, S. Neumeier, M. Göken, Thermophysical and mechanical properties of advanced single crystalline Co-base superalloys, Metall. Mater. Trans. A 49 (9) (2018) 4099–4109.
[35] P. Pandey, A.K. Sawant, B. Nithin, Z. Peng, S.K. Makineni, B. Gault, K. Chattopadhyay, On the effect of Re addition on microstructural evolution of a CoNi-based superalloy, Acta Mater. 168 (2019) 37–51.
[36] C.H. Zenk, S. Neumeier, H.J. Stone, M. Goken, Mechanical properties and lattice misfit of γ/γ′ strengthened Co-base superalloys in the Co-W-Al-Ti quaternary system, Intermetallics 55 (55) (2014) 28–39.
[37] K.E. Yoon, R.D. Noebe, D.N. Seidman, Effects of rhenium addition on the temporal evolution of the nanostructure and chemistry of a model Ni-Cr-Al superalloy. I: experimental observations, Acta Mater. 55 (2007) 1145–1157.
[38] K.E. Yoon, R.D. Noebe, D.N. Seidman, Effects of rhenium addition on the temporal evolution of the nanostructure and chemistry of a model Ni-Cr-Al superalloy. II: analysis of the coarsening behavior, Acta Mater. 55 (2007) 1159–1169.
[39] C. Booth-Morrison, J. Weninger, C.K. Sudbrack, Z. Mao, R.D. Noebe, D.N. Seidman, Effects of solute concentrations on kinetic pathways in Ni-Al-Cr alloys, Acta Mater. 56 (2008) 3422–3438.
[40] V.A. Vorontsov, J.S. Barnard, K.M. Rahman, H.-Y. Yan, P.A. Midgley, D. Dye, Coarsening behaviour and interfacial structure of γ′ precipitates in Co-Al-W based superalloys, Acta Mater. 120 (2016) 14–23.
[41] H.J. Zhou, F. Xue, H. Chang, Q. Feng, Effect of Mo on microstructural characteristics and coarsening kinetics of γ′ precipitates in Co-Al-W-Ta-Ti alloys, J. Mater. Sci. Technol. 34 (2018) 799–805.
[42] A.J. Ardell, R.B. Nicholson, On the modulated structure of aged Ni-Al alloys: with an Appendix on the elastic interaction between inclusions by J. D. Eshelby, Acta Metall. 14 (10) (1966) 1295–1309.
[43] S. Meher, S. Nag, J. Tiley, A. Goel, R. Banerjee, Coarsening kinetics of γ′ precipitates in cobalt-base alloys, Acta Mater. 61 (11) (2013) 4266–4276.
[44] D.J. Chellman, A.J. Ardell, The coarsening of γ′ precipitates at large volume fractions, Acta Metall. 22 (1974) 577–588.
[45] W.Z. Wang, T. Jin, J.L. Liu, X.F. Sun, H.R. Guan, Z.Q. Hu, Role of Re and Co on microstructures and γ′ coarsening in single crystal superalloys, Mater. Sci. Eng. A 479 (2008) 148–156.
[46] A. Suzuki, G.C. DeNolf, T.M. Pollock, Flow stress anomalies in γ/γ′ two-phase Co-Al-W-base alloys, Scr. Mater. 56 (5) (2007) 385–388.
[47] R.W. Kozar, A. Suzuki, W.W. Milligan, J.J. Schirra, M.F. Savage, T.M. Pollock, Strengthening mechanisms in polycrystalline multimodal nickel-base superalloys, Metall. Mater. Trans. A 40 (7) (2009) 1588–1603.
[48] S.K. Makineni, B. Nithin, K. Chattopadhyay, Synthesis of a new tungsten-free γ-γ′ cobalt-based superalloy by tuningalloying additions, Acta Mater. 85 (2015) 85–94.